

Localization of Flavonoids in Seeds by Cluster Time-of-Flight Secondary Ion Mass Spectrometry Imaging

Alexandre Seyer,[†] Jacques Einhorn,^{‡,§} Alain Brunelle,^{*,†} and Olivier Laprévote^{†,||}

Centre de recherche de Gif, Institut de Chimie des Substances Naturelles, CNRS, Avenue de la Terrasse, F-91198 Gif-sur-Yvette, Unité de Phytopharmacie et Médiateurs Chimiques and Unité de Biologie Cellulaire, INRA, route de St-Cyr, 78026 Versailles, France, and Laboratoire de Toxicologie, IFR 71, Faculté des Sciences Pharmaceutiques et Biologiques, Université Paris Descartes, 4 avenue de l'Observatoire, 75006 Paris, France

Time-of-flight secondary ion mass spectrometry imaging has been used to map flavonoids in fresh seed sections of peas (*Pisum sativum*) and *Arabidopsis thaliana*. While for peas a very simple preparation method derived from mammalian tissue imaging could be utilized, several preparation methods had to be tested for the *A. thaliana* seeds before obtaining tissue sections on which the diagnostic ions were not delocalized. For such small and stiff biological material, none of the methods currently used in histology or scanning electron microscopy could be transferred to mass spectrometry imaging. Only the embedding of the fresh seeds in a polyester resin, followed by the analysis of the block after having obtained a flat surface section with a diamond blade, gave sensitive and reproducible results. Several flavonoid ions have been detected in the sections, showing increased concentrations of flavonoids in the seed coats. The method was finally applied to confirm the variations in the flavonoid content of seeds from different *A. thaliana* mutants.

Flavonoids are plant secondary metabolites that originate from the phenylpropanoid biosynthesis pathway. These compounds are widely distributed in plants and have numerous functions, such as flower pigmentation and protection against bacterial or insect attacks.¹ It has been suggested by epidemiologic and laboratory studies that flavonoids have a beneficial effect on human health, in preventing the occurrence of aging-linked diseases such as cardiovascular diseases^{2,3} and some cancers.⁴ This explains the increasing interest brought to a better understanding of flavonoid accumulation and metabolism. The polyphenol content of two kinds of seeds, *Pisum sativum* and *Arabidopsis thaliana*, has

recently been extensively studied.^{5,6} Quantitative electrospray ionization liquid chromatography–mass spectrometry (ESI-LC–MS) measurements were done showing some differences in concentrations between seed coat and cotyledon extracts. The analysis of flavonoids by tandem mass spectrometry (MS–MS) and nuclear magnetic resonance (NMR) has recently been reviewed.⁷

Among the various techniques aiming to map the surface of a sample, mass spectrometry imaging (MSI) is the only one that provides a view of the spatial localization of numerous chemical compounds within a single analysis.⁸ Contrary to other methods such as immunohistochemistry or fluorescence microscopy, for which the molecules of interest need to be labeled before the experiment, MSI is not limited to any a priori knowledge of the molecules. Three different methods coexist that have different advantages and drawbacks: time-of-flight secondary ion mass spectrometry (TOF-SIMS), matrix-assisted laser desorption ionization (MALDI), and nano-SIMS. While MALDI, which is the most popular molecular imaging method, aims to localize peptides and proteins, but also lipids and metabolites, at a resolution of a few tens of micrometers ($\sim 50 \mu\text{m}$) at the surface of the sample,⁹ the so-called nano-SIMS gives very precise localization of elements or small fragments at a scale of a few tens of nanometers only.¹⁰ Between these two extremes, TOF-SIMS is able to localize various molecules, mainly lipids and metabolites, with a mass-to-charge ratio up to m/z 1000–1500 and a routine resolution from 400 nm to 1–2 μm . Thanks to the great increase of sensitivity brought by new polyatomic ion sources,^{11–13} TOF-SIMS imaging has been for several years much more widely utilized in animal and human

* To whom correspondence should be addressed. E-mail: Alain.Brunelle@icsn.cnrs-gif.fr. Phone 33 169 824 575. Fax: 33 169 077 247.

[†] CNRS.

[‡] Unité de Phytopharmacie et Médiateurs Chimiques, INRA.

[§] Unité de Biologie Cellulaire, INRA.

^{||} Université Paris Descartes.

- (1) Dixon, R. A.; Achine, L.; Kota, P.; Liu, C. J.; Reddy, M. S. S.; Wang, L. J. *Mol. Plant Pathol.* **2002**, 3, 371–390.
- (2) Bagchi, D.; Sen, C. K.; Ray, S. D.; Das, D. K.; Bagchi, M.; Preuss, H. G.; Vinson, J. A. *Mutat. Res.* **2003**, 523–524, 87–97.
- (3) Serafini, M.; Bugianesi, R.; Maiani, G.; Valtuena, S.; De Santis, S.; Crozier, A. *Nature* **2003**, 424, 1013.
- (4) Park, O. J.; Surh, Y. J. *Toxicol. Lett.* **2004**, 150, 43–56.

- (5) Dueñas, M.; Estrella, I.; Hernández, T. *Eur. Food Res. Technol.* **2004**, 219, 116–123.
- (6) Routaboul, J. M.; Kerhoas, L.; Debeaujon, I.; Pourcel, L.; Caboche, M.; Einhorn, J.; Lepiniec, L. *Planta* **2006**, 224, 96–107.
- (7) March, R.; Brodbelt, J. J. *Mass Spectrom.* **2008**, 43, 1581–1617.
- (8) McDonnell, L. A.; Heeren, R. M. A. *Mass Spectrom. Rev.* **2007**, 26, 606–643.
- (9) Cornett, D. S.; Reyzer, M. L.; Chaurand, P.; Caprioli, R. M. *Nat. Methods* **2007**, 4, 828–833.
- (10) Guerquin-Kern, J. L.; Wu, T. D.; Quintana, C.; Croisy, A. *Biochim. Biophys. Acta* **2005**, 1724, 228–238.
- (11) Touboul, D.; Halgand, F.; Brunelle, A.; Kersting, R.; Tallarak, E.; Hagenhoff, B.; Laprévote, O. *Anal. Chem.* **2004**, 76, 1550–1559.
- (12) Sjövall, P.; Lausmaa, J.; Johansson, B. *Anal. Chem.* **2004**, 76, 4271–4278.
- (13) Weibel, D.; Wong, S.; Lockyer, N.; Blenkinsopp, P.; Hill, R.; Vickerman, J. C. *Anal. Chem.* **2003**, 75, 1754–1764.

biology.^{14–16} The possibility to map ions at the surface of vegetal tissues has been nevertheless seldomly explored by this method,¹⁷ while a few studies based on MALDI or LDI (laser desorption ionization) have been reported. Wheat seeds have been mapped by MALDI.¹⁸ Atmospheric pressure infrared MALDI (AP-IR-MALDI) was used for an extensive study of the composition in flavonoids and other compounds, as well as their localization, in lily flowers, fruits, leaves, almond seeds, and bulbs.¹⁹ LDI using colloidal graphite as a matrix was also utilized to map flavonoids in flower petals, leaves, and stems of *A. thaliana*.²⁰ In the present work we have used TOF-SIMS imaging to map ions from flavonoids, such as kaempferol and quercetin glycosides, in seeds of extremely different sizes. Pea seeds (*P. sativum*), having a section of up to 10 mm, have first been mapped, and in a second step seeds of *A. thaliana*, with a typical size of ~400 μm or less, were investigated. *A. thaliana* is a model plant for the study of biosynthesis and regulation of the flavonoid pathway, due to the availability of a wide range of mutants affected in this pathway.²¹ Sample preparation was undoubtedly the most delicate step. In contrast to MALDI-TOF imaging, no coating of the sample is needed for TOF-SIMS or nano-SIMS imaging. However, it was required to obtain a rigorously flat and nonpolluted surface. Due to their very small size, it was of special importance to ensure the nondelocalization of the metabolites of interest in seeds of *A. thaliana*. Several methods were thus explored in this study to obtain a suitable procedure.

MATERIALS AND METHODS

Chemicals. Flavonoid standards of kaempferol (MW 286.05), quercetin (MW 302.04), isoquercetin (MW 464.10), quercetin 3-O-rutinoside (MW 610.15), quercetin 3-O-rhamnoside (MW 448.10), kaempferol 3-O-rutinoside (MW 594.16), and kaempferol 3-O-glucoside (MW 448.10) and lipid standards of triacylglycerols (TAGs) 14:0/14:0/14:0 (TAG42:0; MW 722.64) and 18:0/18:0/16:0 (TAG52:0; MW 862.80) and phosphatidylinositol 16:0/18:2 (PI34:2; MW 834.53) were purchased from Sigma-Aldrich (BP 701, F-38297 St-Quentin-Fallavier, France). Structures of some of these flavonoids are shown in Figures S-1 and S-2 (Supporting Information). To record spectra of these standard compounds, 0.5 μL of each solution (0.5 mg·mL⁻¹ in methanol/water (50:50, v/v)) was deposited onto a silicon wafer, the droplet of several square millimeters was allowed to dry, and a surface of 500 $\mu\text{m} \times$ 500 μm inside this dried droplet was scanned by the primary ion beam with a fluence of ~3.6 \times 10¹⁰ ions·cm⁻². Dilutions were also carried out to determine the limits of detection.

Plant Seeds. The wild type and tt7 and tt4 mutants of *A. thaliana* seeds were obtained from the INRA-Versailles collection. Plants were grown in a controlled growth chamber with a 16 h photoperiod. Seeds were collected after a ca. 18 day maturation

period. Seeds from *P. sativum* NGB 5839 variety were also provided by INRA-Versailles. *P. sativum* seeds of the ZP-840 variety were graciously provided by M. Dueñas (CSIC, Madrid, Spain). The NGB variety is often used for physiological studies due to its small size and great convenience for handling, whereas the latter (cultivated by the Instituto Agrario of Valladolid, Spain) yielding dark seeds was known as potentially rich in flavonoids.

Sample Preparation. The sample preparation from a dry or fresh seed is rather difficult. Furthermore, some parts, such as the coat and the cotyledon, may have different levels of hardness. Testing procedures on *A. thaliana* seeds were extremely delicate and challenging due to their very small size. The two varieties of peas, ZP 840 and NGB 5839, were received fresh in the laboratory and immediately frozen at -80 °C. Sections 12 μm thick were cut at -20 °C with a cryostat (CM3050-S, Leica Microsystèmes SA, Nanterre, France) and deposited onto silicon wafers (2 in. diameter polished silicon wafers, ACM, Villiers-Saint-Fréderic, France). Samples were dried just before analysis under a pressure of a few hectopascals for 15 min, without any further treatment. This procedure is exactly the same as that routinely used in the laboratory for mammalian tissue imaging.²² Reference images of sections (not shown) were taken with an Olympus BX51 microscope (Rungis, France), equipped with 1.25 \times to 50 \times lenses and a Color View I camera, monitored by Cell^B software (Soft Imaging System GmbH, Münster, Germany).

Wild-type (WT) *A. thaliana* seeds were first prepared according to established sample preparation procedures for histology and/or scanning electron microscopy at INRA-Versailles. These methods gave negative results. The method that was finally used was adapted from that described for imaging in cultural heritage samples. Details are given in the Results and Discussion.

TOF-SIMS Imaging Data Acquisition and Processing. The experiments were performed using a commercial TOF-SIMS IV spectrometer (Ion-ToF GmbH, Münster, Germany), located at the Institut de Chimie des Substances Naturelles (Gif-sur-Yvette, France). The spectrometer is equipped with a liquid metal ion gun (LMIG) filled with bismuth, and Bi₃⁺ ions have always been selected, as they provide, among all the other bismuth cluster species, the best compromise between intensity and efficiency.²³ Primary ions reach the sample surface with a kinetic energy of 25 keV and at an angle of incidence of 45°. The fluence (also called primary ion dose density) is maintained between 2 \times 10¹¹ and 2 \times 10¹² ions·cm⁻², which is always below the so-called static SIMS limit.²⁴ Secondary ions are accelerated to an energy of 2 keV, fly through a field-free region, and are reflected (effective flight path ~2 m) before being postaccelerated to 10 keV just before hitting the entrance surface of the hybrid detector, which is made of one microchannel plate, a scintillator, and a photomultiplier. A low-energy electron flood gun is activated between two primary ions pulses to neutralize the sample surface with the minimum damage.²⁵ Two modes of operation of the primary ion column have been used during

- (14) Brunelle, A.; Laprévote, O. *Curr. Pharm. Des.* **2007**, *13*, 3335–3343.
- (15) Nygren, H.; Malmberg, P. *Trends Biotechnol.* **2007**, *25*, 499–504.
- (16) Brunelle, A.; Laprévote, O. *Anal. Bioanal. Chem.* **2009**, *393*, 31–35.
- (17) Tokareva, E. N.; Fardim, P.; Pranovich, A. V.; Fagerholm, H. P.; Daniel, G.; Holmbom, B. *Appl. Surf. Sci.* **2007**, *253*, 7569–7577.
- (18) Burrell, M. M.; Earnshaw, C. J.; Clench, M. R. *J. Exp. Bot.* **2007**, *58*, 757–763.
- (19) Li, Y.; Shrestha, B.; Vertes, A. *Anal. Chem.* **2008**, *80*, 407–420.
- (20) Cha, S.; Zhang, H.; Ilarslan, H. L.; Surkin Wurtele, E.; Brachova, L.; Nikolau, B. J.; Yeung, E. S. *Plant J.* **2008**, *55*, 348–360.
- (21) Winkel-Shirley, B. *Plant Physiol.* **2001**, *126*, 485–493.

- (22) Brunelle, A.; Touboul, D.; Laprévote, O. *J. Mass Spectrom.* **2005**, *40*, 985–999.
- (23) Touboul, D.; Kollmer, F.; Niehuis, E.; Brunelle, A.; Laprévote, O. *J. Am. Soc. Mass Spectrom.* **2005**, *16*, 1608–1618.
- (24) Vickerman, J. C. TOF-SIMS—an overview. In *ToF-SIMS—Surface Analysis by Mass Spectrometry*; Vickerman, J. C., Briggs, D., Eds.; Surface Spectra and IM Publications: Manchester and Chichester, U.K., 2001; pp 1–40.
- (25) Gilmore, I. S.; Seah, M. P. *Appl. Surf. Sci.* **2002**, *187*, 89–100.

the experiments. The first one, which is called “high-current bunched mode”, ensures both a beam focus of $2\text{ }\mu\text{m}$ and a pulse duration of less than 1 ns, thus enabling an excellent mass resolution, $M/\Delta M = 8 \times 10^3$ (fwhm), at m/z 500. For the second operating mode, which is called “burst alignment”, the primary ion beam focus diameter is ~ 400 nm, but the primary ion pulses cannot be bunched, and the pulse duration is 20–100 ns, ensuring only a nominal mass resolution. A detailed description of the different setting modes of the ion column can be found elsewhere.²⁶ The Bi_3^+ primary ion current, measured at 10 kHz with a Faraday cup on the grounded sample holder, is ~ 0.4 pA in the high-current bunched mode and 0.05 pA in the burst alignment mode.

Two modes of image acquisition have been used. Images of *A. thaliana* seed sections, with fields of view of $500\text{ }\mu\text{m} \times 500\text{ }\mu\text{m}$ or less, were recorded without sample stage movement just by rastering the primary ion beam. For most of these images, the high-current bunched mode (see above) was preferred. The number of pixels was chosen as 256×256 to obtain a $2\text{ }\mu\text{m}$ or less pixel size. The burst alignment ion gun mode was used when a higher image resolution was needed. In this case the image was acquired with a field of view of $150\text{ }\mu\text{m} \times 150\text{ }\mu\text{m}$ and a ~ 600 nm pixel size (256×256 pixels). For images of *P. sativum* sections, a large-area analysis ($9.1\text{ mm} \times 9.1\text{ mm}$) was performed using the same LMIG conditions (high-current bunched mode) and the so-called stage scan. In this case, the sample is continuously moved by the sample stage. The repeatability of the movement is better than $5\text{ }\mu\text{m}$. To scan the whole surface area, the primary ion beam is rastered over the area of each individual pixel. The number of pixels was 256×256 , each pixel having a size of ~ 35 μm . In these conditions, the fluence was 6.7×10^9 ions $\cdot \text{cm}^{-2}$.

Because of the very low initial kinetic energy distribution of the secondary ions, the relationship between the time-of-flight and the square root of m/z is always linear over the whole mass range. The mass calibration was always internal, and signals used for initial calibration were those of H^+ , H_2^+ , H_3^+ , C^+ , CH^+ , CH_2^+ , CH_3^+ , and C_2H_5^+ for the positive ion mode and those of C^- , CH^- , C_2^- , and C_2H^- for the negative ion mode.

The name of the compound or the m/z value of the peak centroid, the maximal number of counts in a pixel (mc), and the total number of counts (tc) are written below each image. The color scales correspond to the $[0, \text{mc}]$ intervals.

Regions of interest (ROIs) corresponding to different image areas were drawn with the IonImage software (Ion-Tof GmbH). The associated mass spectra were further extracted to reveal different local compositions. For a proper and easier comparison, as each ROI had a different area (in pixels), a normalization of their respective mass spectrum intensities had to be performed. The intensity of the mass spectrum from each ROI was normalized against the area of the smallest one.

RESULTS AND DISCUSSION

Mass Spectrometry Analysis of Flavonoid Standards. It is important to record reference mass spectra of pure standard compounds, in parallel to the imaging experiments, to help and reinforce the mass assignments. Studies with the TOF-SIMS instrument have been performed first in the positive ionization mode, but the negative one appeared the most sensitive and

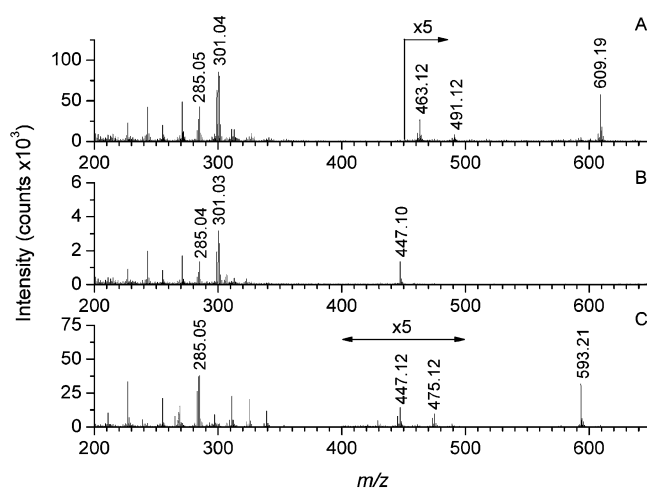


Figure 1. TOF-SIMS negative ion mass spectra of quercetin 3-O-rutinoside (A), quercetin 3-O-rhamnoside (B), and kaempferol 3-O-rutinoside (C).

convenient for identification. Figure 1 shows the TOF-SIMS negative ion mass spectra of quercetin 3-O-rutinoside (MW 610.15; Figure 1A), quercetin 3-O-rhamnoside (MW 448.10; Figure 1B), and kaempferol 3-O-rutinoside (MW 594.16; Figure 1C). The signal of the deprotonated molecule $[\text{M} - \text{H}]^-$ is well detected in each spectrum (at m/z 609.19, 447.1, and 593.21, respectively), while intense fragment ion peaks are detected particularly near the aglycon ion region at m/z 301.04 and 285.05, respectively. Much less abundant ions can also be noticed in the intermediate region of Figure 1A,C (at m/z 463.12 and 447.12, respectively), which likely correspond to the loss of the external rhamnosyl (146 u) sugar of the glycosidic chain from $[\text{M} - \text{H}]^-$. The nomenclature of these fragmentations is recalled in Figure S-2 (Supporting Information), according to Kerhoas et al.²⁷ A careful examination of spectra of the monoglycosides quercetin 3-O-rhamnoside and quercetin 3-O-glucoside and of the diglycoside quercetin 3-O-rutinoside at various concentrations (0.5–500 ng deposited amounts) led to systematic observation of a triplet of ions of similar abundances in the aglycon ion region. This observation indicates that the mono- or disaccharide moiety can be eliminated by three competitive pathways, yielding ions $[\text{M} - \text{H} - \text{Gly}]^-$, $[\text{M} - \text{H} - \text{GlyH}^\bullet]^{+/-}$, and $[\text{M} - \text{H} - \text{GlyH}_2]^-$, at m/z 301.03, 300.03, and 299.03, respectively, for the quercetin series. The same behavior was found in the kaempferol series (data not shown). This type of fragmentation is to some extent more complex than that observed under ESI-MS–MS using low-energy collision-activated dissociation of the $[\text{M} - \text{H}]^-$ ion.²⁷ The limit of detection of such compounds was found to be 2–3 ng deposited amount ($\text{S}/\text{N} = 3$). In the study of Kerhoas et al.,²⁷ the authors have taken advantage of tandem mass spectrometry to identify the main flavonoid fragments from *A. thaliana* seeds. With the TOF-SIMS IV spectrometer, it is not possible to perform tandem mass spectrometry. Although postsource decay like experiments can in some cases be carried out,²⁸ this method does not generally enable the complete structural analysis of ions. It was thus also important for unambiguous

(27) Kerhoas, L.; Aouak, D.; Cingöz, A.; Routaboul, J. M.; Lepiniec, L.; Einhorn, J.; Birlirakis, N. *J. Agric. Food Chem.* 2006, 54, 6603–6612.

(28) Touboul, D.; Brunelle, A.; Laprevôte, O. *Rapid Commun. Mass Spectrom.* 2006, 20, 703–709.

ion assignments to consider in the present study other criteria such as isotopic patterns, colocalization (or not) of ion images, and information from previous conventional work.

Sample Preparation from Seeds and Time-of-Flight Analyzer Settings. In the case of *P. sativum* seeds, the same preparation method as for animal tissues, i.e., inclusion in OCT (optimum cutting temperature) glue and sectioning at -20°C in a cryostat, appeared simple and convenient for such large size samples. However, *A. thaliana* seeds are small size samples of $\sim 0.4\text{ mm}$ dimension, and for which a robust and reproducible preparation method had therefore to be found. Several fixation methods, which are popular in histology, have been tested first, followed by cross sections using stainless steel or diamond blades. Inclusion in OCT glue and cryosectioning was also tested. Finally, cross sections of seeds embedded in a polyester resin have been obtained using an ultramicrotome equipped with a diamond blade. This last method was found to be the most suitable and reproducible one among all tested procedures.

The seeds (WT) were first fixed in formaldehyde, then dried in several successive ethanol baths, and finally placed in four different embedding materials, wax, paraffin, and two different resins currently utilized in histology, an epoxy resin (Spurr) and a glycol methacrylate resin (historesin). Other WT fresh seeds were frozen at -80°C . For those seeds, two different preparation methods have been utilized. Some have been embedded in OCT glue, without any preliminary treatment. The glue was allowed to harden at -30°C , and $30\text{ }\mu\text{m}$ thick sections were prepared at a temperature of -20°C with the Leica cryostat, deposited onto silicon wafers, and finally dried under a pressure of a few hectopascals for 15 min, without any further treatment, just before analysis. In a last attempt, fresh seeds were defrosted and embedded in a polyester resin (H59, Sodem, France). The resin block was polished until the sample reached the surface and then cut into 500 nm thick sections by ultramicrotomy using a Diatome diamond blade (Leica Microsystèmes). Due to the impossibility to maintain these sections intact, the analyses were performed directly on the flat and clean surface of the block itself.

For the seeds embedded in epoxy (Spurr) and glycol methacrylate (historesin) resins (data not shown), most of the detected ions originated from lipids. Ions at m/z 285.07, 301.07, and 447.10, which can be attributed to flavonoids (see above), were also detected, but appeared mainly in the embedding resin and thus delocalized by the sample preparation. When using wax or paraffin, no ions that could originate from the seed were detected. These methods utilizing fixation and dehydration prior to the embedding step are therefore not adapted for TOF-SIMS mass spectrometry imaging. When the fresh seeds were embedded in OCT glue, it was very difficult to obtain a section that was not covered by a thin glue layer. The mass spectra obtained from 30 different sections were almost all dominated by OCT glue ions. Only one section was usable for mass spectrometry imaging, yielding ions at m/z 285.07, 301.07, and 447.10 in the seed tissue itself (data not shown). Thus, embedding the *A. thaliana* seeds in OCT glue could not be considered as a reproducible sample preparation method.

Finally, the embedding in a polyester resin, followed by cutting with an ultramicrotome, a procedure already utilized to analyze

cross sections of cultural heritage samples,²⁹ was successfully tested in the present study. The obtained seed sections were flat and did not exhibit any noticeable pollution in the mass spectra. Nevertheless, such samples made of a 6–8 mm thick block of resin are not conductive and, when introduced into the electrostatic field set to extract the secondary ions, behave like a dielectric at the surface of which the voltage cannot be known in advance. The consequence is that the kinetic energy of the secondary ions is not exactly 2 keV, but a fixed but indeterminate value, between 0 and 2 keV. Without any correction of the secondary ion optics, the reflectron and lenses along the ion path would not be correctly tuned and the ion trajectories would not be correct, leading to bad mass resolution and ion transmission. A simple and efficient way to adjust the parameters of the analyzer to the effective kinetic energy of the secondary ions is to take advantage of the capability of a reflectron to be used to measure this kinetic energy. Indeed, by decreasing the voltage applied to the end electrode of the reflectron, the value for which the ion signals vanish from the spectra is, if multiplied by the charge of the ions, equal to their kinetic energy. Then it is easy to tune all the analyzer voltages according to this new value of the kinetic energy. This method for an optimized tuning of the analyzer parameters, which is called by the manufacturer the “charge compensation mode”, enables a mass resolution quite as high as for conductive samples to be reached, with an excellent ion transmission. This step cannot be neglected for such samples, since the measured kinetic energy defect is in the present case $\sim 10\%$ (whatever the polarity, the true kinetic energy of the secondary ions is $\sim 1.8\text{ keV}$ instead of 2 keV, for $\pm 2\text{ kV}$ applied), while it is only $\sim 1\%$ or less for thin mammalian tissue sections.

Flavonoid Imaging in Seeds of *P. sativum*. Since flavonoids are better detected in the negative ion mode than in the positive ion mode, we have chosen to focus our study on negative ion spectra and images. The total negative ion mass spectrum recorded at the surface of a section of a ZP-840 pea seed is shown in Figure S-3 (Supporting Information). This spectrum is dominated by lipid ion peaks: carboxylate ions of palmitic acid (C16:0 ; m/z 255.2) and of linoleic acid (C18:2 ; m/z 279.2) and deprotonated molecules of triacylglycerols [$\text{TAG42:0} - \text{H}]^-$ (m/z 721.5) and [$\text{TAG52:0} - \text{H}]^-$ (m/z 861.5) and of phosphatidylinositol [$\text{PI34:2} - \text{H}]^-$ (m/z 833.5). Many noncharacteristic fragment ions are observed below m/z 200. Reference mass spectra of the most abundant lipids detected in the negative ion mode have also been recorded in parallel (triacylglycerols TAG42:0 and TAG52:0 and phosphatidylinositol PI34:2, data not shown).

Figures 2 and 3 show the localization of various phenolics and flavonoids previously analyzed by ESI-LC–MS in the two varieties of peas ZP 840 and NGB 5839, respectively.⁵ Dueñas et al. have compared the polyphenol content of the cotyledon and of the seed coat of two different pea varieties, ZP-840 and *Fidelia*. According to the identification of four different areas on the sample surface, namely, the cotyledon, radicle, seed coat, and seed coat near the radicle, evidenced in Figures 2G and 3G, Table 1 summarizes the localizations of several ions detected in these areas. For the ZP-840 variety, ions at m/z 153.03 and 288.98 are localized in the same areas as those identified by Dueñas et al. The ion at m/z

(29) Mazel, V.; Richardin, P.; Touboul, D.; Brunelle, A.; Walter, P.; Laprévote, O. *Anal. Chim. Acta* 2006, 570, 34–40.

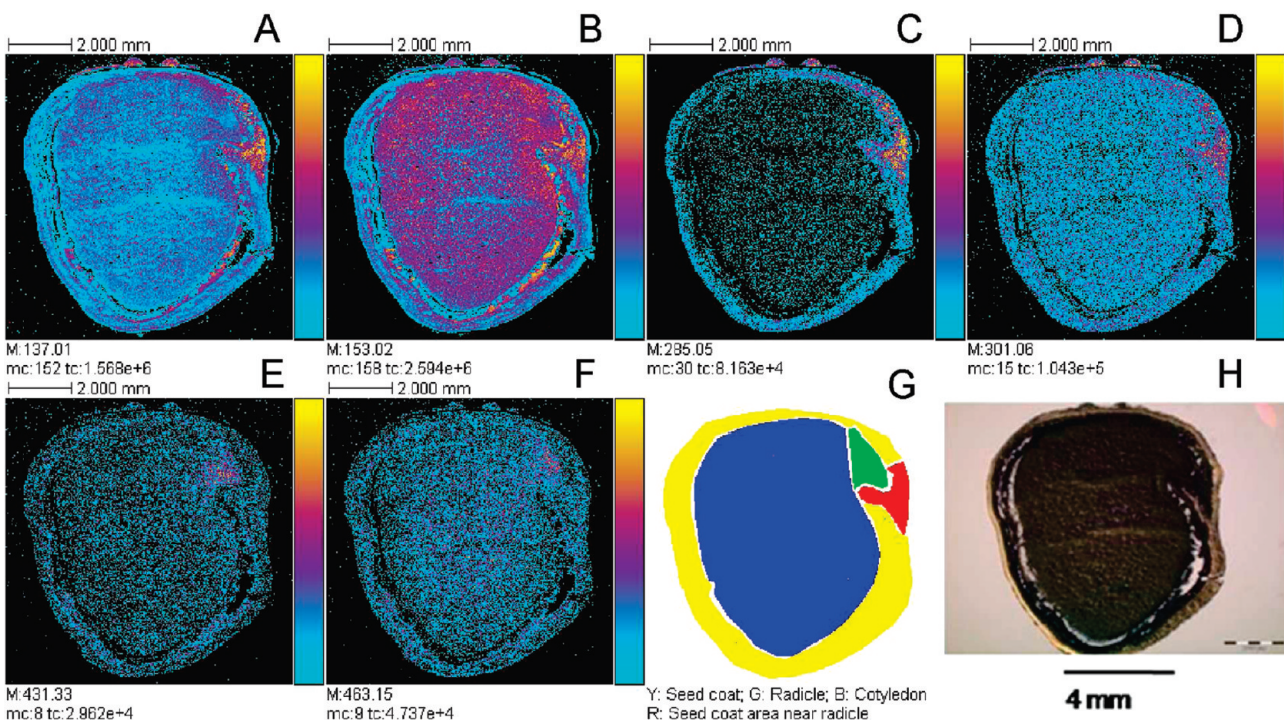


Figure 2. TOF-SIMS negative ion images of a *P. sativum* ZP-840 tissue section: (A) *p*-hydroxybenzoic acid (m/z 137.01); (B) protocatechuic acid or gallic aldehyde (m/z 153.02); (C) flavonoid fragment (kaempferol at m/z 285.05); (D) flavonoid fragment (quercetin at m/z 301.06); (E) apigenin glycoside or other (m/z 431.33); (F) quercetin 3-O-galactoside (m/z 463.15); (G) ROIs showing in yellow the seed coat, in green the radicle, in blue the cotyledon, and in red the seed coat area near the radicle; (H) optical image (field of view 9.1 mm \times 9.1 mm, 256 \times 256 pixels, pixel size 35.54 μm , fluence $6.7 \times 10^9 \text{ ions}\cdot\text{cm}^{-2}$). Color scale bars, with amplitude in number of counts, are indicated to the right of each ion image. The amplitude of the color scale corresponds to the maximum number of counts (mc) and could be read as [0, mc]. tc is the total number of counts recorded for the specified m/z (sum of counts in all the pixels).

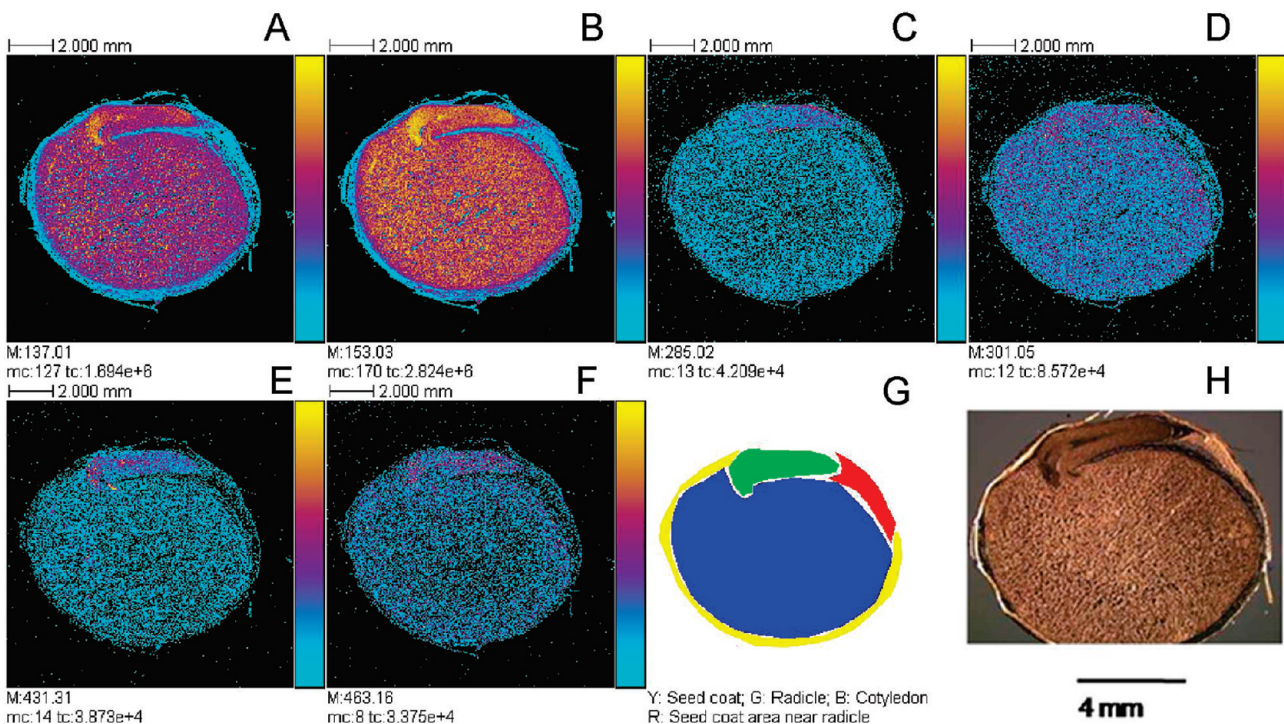


Figure 3. TOF-SIMS negative ion images of a *P. sativum* NGB 5839 tissue section: (A) *p*-hydroxybenzoic acid (m/z 137.00); (B) protocatechuic acid or gallic aldehyde (m/z 153.03); (C) flavonoid fragment (kaempferol at m/z 285.02); (D) flavonoid fragment (quercetin at m/z 301.05); (E) apigenin glycoside or other (m/z 431.31); (F) quercetin 3-O-galactoside (m/z 463.16); (G) ROIs showing in yellow the seed coat, in green the radicle, in blue the cotyledon, and in red the seed coat area near the radicle; (H) optical image (field of view 13 mm \times 13 mm, 256 \times 256 pixels, pixel size 50.78 μm , fluence $3.86 \times 10^9 \text{ ions}\cdot\text{cm}^{-2}$). Color scale bars, with amplitude in number of counts, are indicated to the right of each ion image. The amplitude of the color scale corresponds to the maximum number of counts (mc) and could be read as [0, mc]. tc is the total number of counts recorded for the specified m/z (sum of counts in all the pixels).

Table 1. Localization of the Main Flavonoids Identified and of Some Precursors^a in the Different Pea Areas^b and for the Two Varieties ZP-840 and NGB-839

possible compound identification	mass to charge ratio (<i>m/z</i>)	<i>m/z</i> difference with exact mass	seed coat	seed coat area near radicle	cotyledon	radicle
ZP 840						
<i>p</i> -hydroxybenzoic acid	137.02	0.00	+	+	+	+
protocatechuic acid or gallic aldehyde	153.03	0.00	+	+	+	+
flavonoid fragment (kaempferol)	285.07	0.02	+	+	—	—
(+)-catechin or (−)-epicatechin	288.98	−0.10	+	+	—	—
flavonoid fragment (quercetin)	301.07	0.03	+	++	++	+
protocatechuic acid glycoside	315.08	0.00	+	+	+	+
apigenin glycoside	431.34	0.24	+	—	—	+
quercetin 3-O-galactoside	463.16	0.06	+	+	+	+
NGB 5839						
<i>p</i> -hydroxybenzoic acid	137.01	−0.01	—	—	+	+
protocatechuic acid or gallic aldehyde	153.03	0.00	+	+	+	+
flavonoid fragment (kaempferol)	285.01	−0.04	—	—	+	++
(+)-catechin or (−)-epicatechin	not detected		—	—	—	—
flavonoid fragment (quercetin)	301.05	0.01	+	+	+	++
protocatechuic acid glycoside	315.08	0.00	—	+	+	++
apigenin glycoside	431.31	0.21	—	—	—	++
quercetin 3-O-galactoside	463.16	0.06	+	+	+	++

^a Key: ++, high; +, present; —, absent. ^b According to schemes in Figures 3G and 4G.

288.98 (deprotonated catechin or epicatechin) is not detected in the NGB 5839 variety, but the ions at *m/z* 153.03 (protocatechuic acid) and 315.08 (protocatechuic acid glycoside) led to similar localizations. The ion at *m/z* 137.02 (*p*-hydroxybenzoic acid) is located at the edge of the cotyledon and in the seed coat area near the radicle of the ZP-840 seed, but only in the cotyledon and radicle for the NGB 5839 variety. An ion at *m/z* 431.34 (Figures 2E and 3E) is detected in TOF-SIMS imaging in the radicle and seed coat for ZP-840 and only in the radicle for NGB 5839. Dueñas et al. attributed an ion at *m/z* 431.0 to an apigenin glycoside that was found in both the cotyledon and the seed coat. However, the important deviation in our study between the observed *m/z* value of this ion and the exact mass calculation as well as its different distribution area makes questionable its assignment as an apigenin derivative. The ion at *m/z* 285.07 (Figures 2C and 3C), which can originate from kaempferol (see above) and eventually from quercetin flavonoids as a minor fragment, is detected in the seed coat and in the area near the radicle for ZP-840 species and around the radical in the NGB 5839 seed. By contrast, the ion at *m/z*

301.07 (Figures 2D and 3D), which can result from the dissociation of quercetin flavonoids only, is detected in the four regions but mainly in the seed coat area near the radicle for ZP-840 and mainly in the radicle for NGB 5839. The ion at *m/z* 463.16 (Figures 2F and 3F) is detected in the seed coat and in the cotyledon, with some accumulation in the radicle. This ion, which is likely to be a deprotonated quercetin glycoside and/or a fragment of a heavier molecular weight quercetin-type compound (di- or triglycoside), was not detected by ESI-LC-MS in the ZP-840 pea (only in the *Fidelia* variety). Inversely, the *m/z* 447.1 ion corresponding to quercetin 3-O-rhamnoside and to a luteolin glycoside is not detected by our imaging approach. Although less phenolic compounds are detected and identified in TOF-SIMS imaging than by ESI-LC-MS, and despite the complexity of the spectra (the high-energy primary ion impacts, responsible for the secondary ion emission, generate intense fragment ion signals), this MSI method generally appears consistent with the results already published in the literature. A few contradictions may, however, be noticed likely if seeds studied by the two approaches are not issued from the same batches. Furthermore, the MSI method provides more detailed localizations of the flavonoid compounds since four different areas (instead of two) showing different relative concentrations could be drawn from the ion images.

Flavonoid Imaging in Seeds of *A. thaliana*. Figure 4 shows the mass spectrum extracted from the ROI of the coat of a wild-type *A. thaliana* seed section. While this spectrum is dominated by signals of fatty acid carboxylates, flavonoid ions at *m/z* 285.04, 301.03, and 447.12 are clearly detected. Figure 5 displays the images of these three ions, which are mainly localized in the seed coat. There is no compound delocalization due to the sample preparation, with respect to the spatial resolution. The flavonoid composition of *A. thaliana* seeds from various origins was studied in detail by Routaboul et al.⁶ The most abundant flavonoid in the wild type was quercetin 3-O-rhamnoside (MW 448.1). Ions *m/z* 447.12 ([M − H][−]) and 301.03 (separated by 146 u, e.g., loss of a rhamnosyl residue) allow characterization of the latter. As seen in the spectrum of the standard, ions at ca. *m/z* 299.05

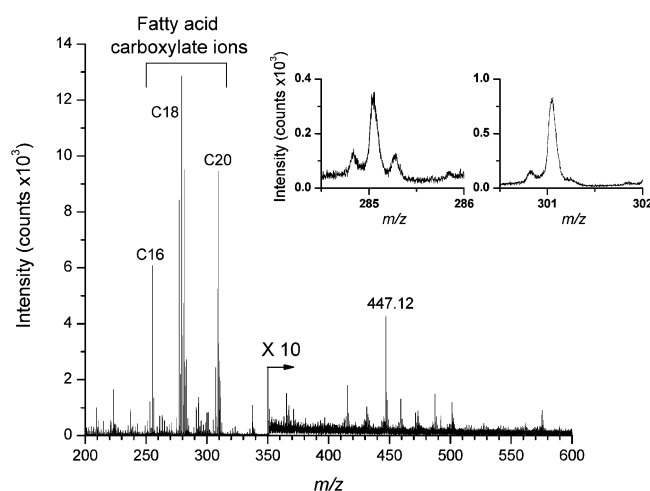


Figure 4. TOF-SIMS negative ion mass spectrum of the area corresponding to the seed coat of an *A. thaliana* seed section embedded in a polyester resin.

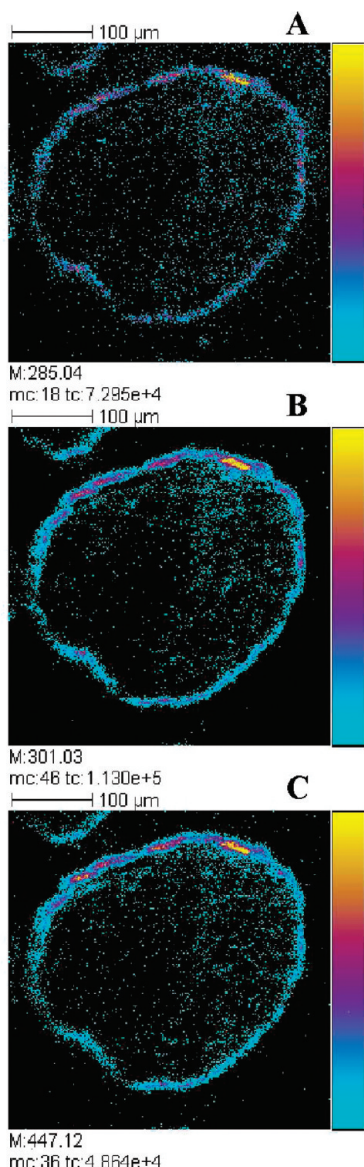
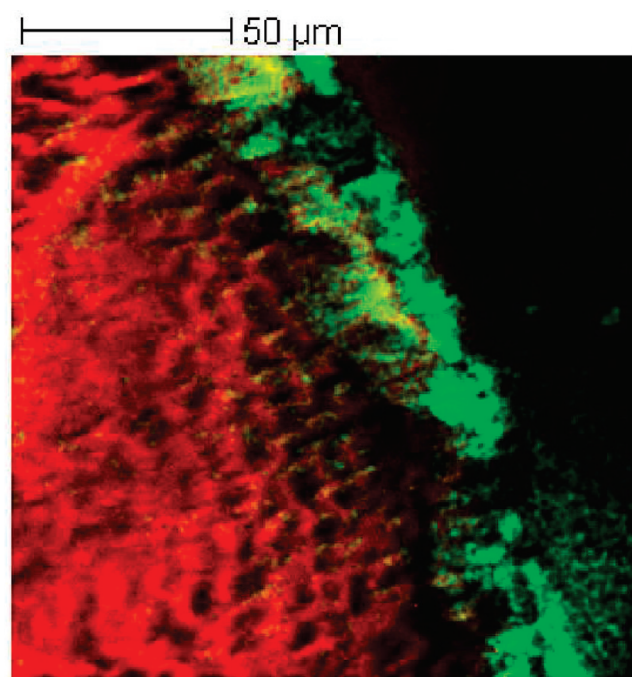


Figure 5. TOF-SIMS negative ion images of an *A. thaliana* seed section, embedded in a polyester resin: (A) m/z 285.04, (B) m/z 301.03, (C) m/z 447.1 (field of view $400\text{ }\mu\text{m} \times 400\text{ }\mu\text{m}$, 256×256 pixels, pixel size $1.56\text{ }\mu\text{m}$, fluence $1.5 \times 10^{12}\text{ ions}\cdot\text{cm}^{-2}$). Color scale bars, with amplitude in number of counts, are indicated to the right of each ion image. The amplitude of the color scale corresponds to the maximum number of counts (mc) and could be read as [0, mc]. tc is the total number of counts recorded for the specified m/z (sum of counts in all the pixels). The ion signals from the coat of another seed section appear in the top left of the images.

and 300.05 resulting from alternative decomposition pathways of the deprotonated molecule might also be considered. These ions at m/z 299.05 and 300.06 may also originate from a phosphoinositol fragment ($\text{C}_9\text{H}_{16}\text{O}_9\text{P}^-$; m/z 299.05) and its ^{13}C contribution (m/z 300.05), respectively. This ambiguity cannot be neglected, and these two ions were not further considered for the analysis of the data. The structure assignment of the ion peak at m/z 285.04 is more ambiguous since it may either originate from a quercetin derivative as a secondary fragment or correspond to a diagnostic ion of kaempferol derivatives. Routaboul et al. found that 90% of quercetin 3-O-rhamnoside was concentrated in the coat while the remaining 10% was



R= Sum of C18
G= Sum of Flavonoids

Figure 6. High spatial resolution negative ion image recorded close to the seed coat of an *A. thaliana* seed section embedded in a polyester resin (field of view $150\text{ }\mu\text{m} \times 150\text{ }\mu\text{m}$, 256×256 pixels, pixel size 586 nm, fluence $4 \times 10^{12}\text{ ions}\cdot\text{cm}^{-2}$). Two-color overlay: red, sum of C18 fatty acid carboxylate ions; green, sum of flavonoid ions.

located in the cotyledon. In the mass spectra extracted from ROIs of the coat and of the cotyledon, the intensity of the $[\text{M} - \text{H}]^-$ ion at m/z 447.12 was 20 times higher in the coat than in the cotyledon. Then the sample preparation method used herein is the one that leads to the most relevant and reproducible results. Furthermore, it was possible with such samples to record an ion image using the high spatial resolution mode (burst alignment). The result, with a pixel size of ~ 600 nm, is shown in Figure 6, which is a color overlay between the sum of C18 fatty acid carboxylate ions (sum of stearic C18:0, oleic C18:1, and linoleic C18:2 fatty acids), in red, and the sum of the three major flavonoid ions detected (m/z 285.04, 301.03, and 447.12), in green. This ion image was recorded at the edge of the seed section, and the coat is clearly represented by the flavonoid ion signals, while the fatty acid ion signals are more intense in the cotyledon. Some small irregularities of the flavonoid ion signal are observed, which could be due either to little variations of the thickness of the seed coat or to alterations of this coat after the contact with the polyester resin during the embedding process of the seed. The other diversely glycosylated flavonoids (the quercetin, kaempferol, and isorhamnetin series) also identified, each representing less than 1–10% of quercetin 3-O-rhamnoside, could not be detected.²⁷

The method was finally tested with seeds from two different mutants (modified in the flavonoid biosynthesis pathway) of *A. thaliana* previously studied by ESI-LC-MS.⁶ A first mutant named tt7 is characterized by the lack of quercetin compounds. A second mutant variety, named tt4, is known to produce no flavonoid. The fresh seeds were prepared using exactly the same procedure as

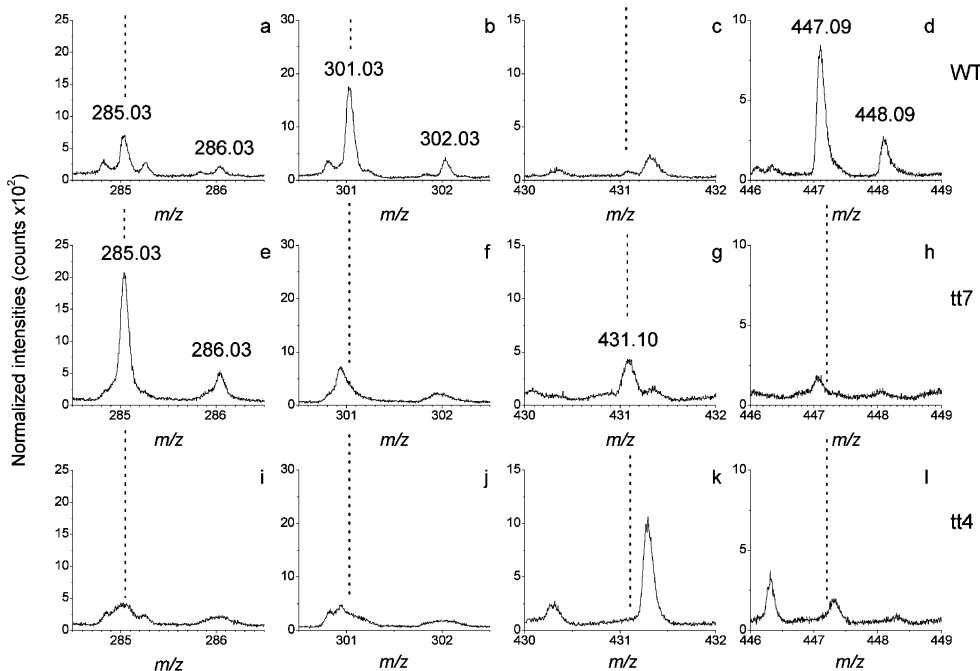


Figure 7. Parts of the TOF-SIMS negative ion mass spectra of the area corresponding to the seed coat of three different *A. thaliana* seeds, the wild type (WT) (a–d) and two different mutants, namely, tt7 (e–h) and tt4 (i–l).

for the wild-type seeds, ion images (not shown) were recorded under the same experimental conditions, and ROIs corresponding to the coat of the three kinds of seeds were drawn to extract the subsequent mass spectra (it was verified that the flavonoids were not detected in the cotyledon areas). These mass spectra are shown in Figure 7 in comparison with that of the WT, and the results obtained are in agreement with the literature.^{6,27} In the wild-type seed, ions at m/z 285.03, 301.03, and 447.09 are detected. Two of them are characteristic of quercetin-type flavonoid (m/z 301.03 and 447.09). None of these ions can be specifically attributed to kaempferol compounds, the presence of which cannot be strictly demonstrated. In the tt7 mutant seed section, ions detected at m/z 285.03 and 431.10 are likely related to kaempferol 3-*O*-rhamnoside and to kaempferol 3,7-di-*O*-rhamnoside, the two major reported flavonoids,²⁷ the parent ion [$M - H^-$] at m/z 577 of the latter not being detected. These observations and the nondetection of a signal for ion m/z 301 allow concluding the presence of only kaempferol-type flavonoids in the tt7 mutant seeds. As also expected, no flavonoid (quercetin and/or kaempferol types) was detected in the tt4 mutant.

CONCLUSION

Cluster TOF-SIMS imaging enables mapping a part of the flavonoid content of pea and *A. thaliana* seed sections. This work needed to select, among various known sample preparation methods, which one could be the best suited for the chemical analysis of such small and hard seeds. While it was relatively easy to prepare the pea sections, since the method was the same as for mammalian tissue sections, none of the methods which are commonly utilized in histology or scanning electron microscopy were found adequate for the chemical imaging of *A. thaliana* seeds by mass spectrometry. It was necessary to embed the seeds in a polyester resin and to cut them with diamond blades in an ultramicrotome. Finally it was possible to localize different classes

of flavonoids, and to confirm the flavonoid content, together with their localization, from mutant types of seeds compared to the wild-type seed. Although that sample preparation method cannot be considered as an easy or rapid one, it is the only one that was found to be reproducible. The same distribution of the major flavonoids was observed through the various wild-type single seeds examined ($n = 10$). According to the literature, that compound is expected to represent less than 0.5% of the total content of a 0.025 mg single seed. In the future, the proposed method could be utilized to map the flavonoid content of *A. thaliana* seeds as a function of their development and maturation and for different mutants and ecotypes. By this way, it is assumed that many more biological features regarding the origin and role of a given flavonoid could be deduced. To improve the detection of minor components, tandem mass spectrometry in association with TOF-SIMS imaging should likely be considered.

ACKNOWLEDGMENT

We thank Jean-Marc Routaboul for providing the *A. thaliana* seeds (WT and mutants) and Adeline Berger, Jocelyne Kronenberger, Pascale Richardin, and Elsa Van Elslande for their help during sample preparation. A.S. is indebted to the Institut de Chimie des Substances Naturelles for a Ph.D. research fellowship. This work was supported by the European Union (Contract LSHG-CT-2005-518194 COMPUTIS).

SUPPORTING INFORMATION AVAILABLE

Additional information as noted in text. This material is available free of charge via the Internet at <http://pubs.acs.org>.

Received for review November 5, 2009. Accepted February 4, 2010.

AC902528T